DIGITAL REPOSITORY FIGURE CAPTIONS

Figure DR1. Location of samples. Labels for most samples within 1 m of fault are omitted for clarity.

Figure DR2. (A) Fission-track length distributions for select samples; 8B-2 and 8F-2 are samples far from fault whereas 8E-1 and 8E-2 are from within 2–4 cm of fault. (B) Photomicrographs of thin sections of corresponding samples. Scale bars are 0.25 mm.

Figure DR3. Forward modeling of thermal history of sample 8B-2 (far from fault, granodiorite side) using AFTSolve (Ketcham et al., 2000) and annealing algorithm of Laslett et al. (1987). The thick red curve shows best fit after a Monte Carlo simulation with 100,000 runs, whereas gray area indicates range of acceptable fits. Modeling shows that our sample locality was at an ambient temperature between 70 and 80 °C while the fault was active.

DIGITAL REPOSITORY REFERENCES CITED

Dumitru, T.A., 1993, A new computer-automated microscope stage system for fission-track analysis, Nuclear Tracks and Radiation Measurements, v. 21, p. 575–580.

Galbraith, R.F., 1981, On statistical-models for fission-track counts, Journal of the International Association for Mathematical Geology, v. 13, p. 471–478.

Green, P.F., 1981, A new look at statistics in fission-track dating, Nuclear Tracks and Radiation Measurements, v. 5, p. 77–86.

Hurford, A.J. and Green, P.F., 1983, The zeta-age calibration of fission-track dating, Isotope Geoscience, v. 1, p. 285–317.

Naeser, C.W., 1979, Fission track dating and geological annealing of fission tracks, in Jaeger, E., and Hunziker, J. C., eds., Lectures in isotope geology: New York, Springer-Verlag, p. 154–169.

Digital Repository Figure DR-1

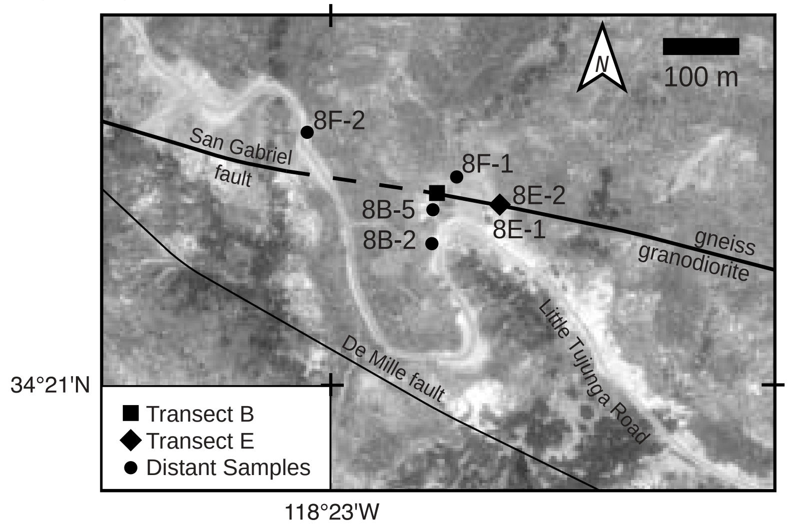

d'Alessio et al., 2003

Digital Repository Figure DR-2

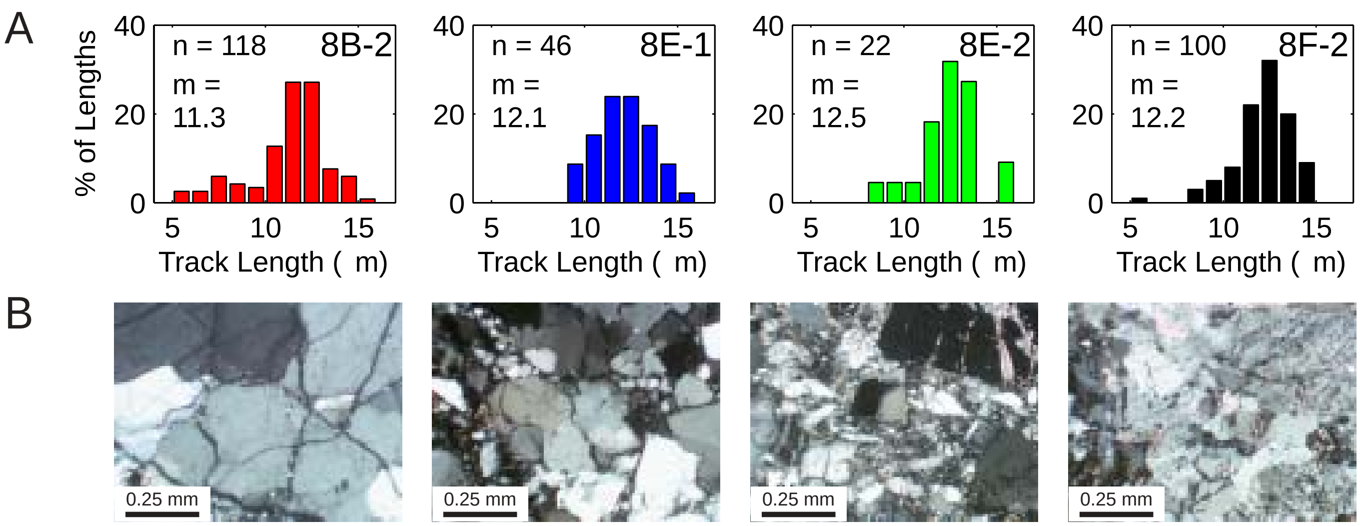

d'Alessio et al., 2003

Digital Repository Figure DR-3

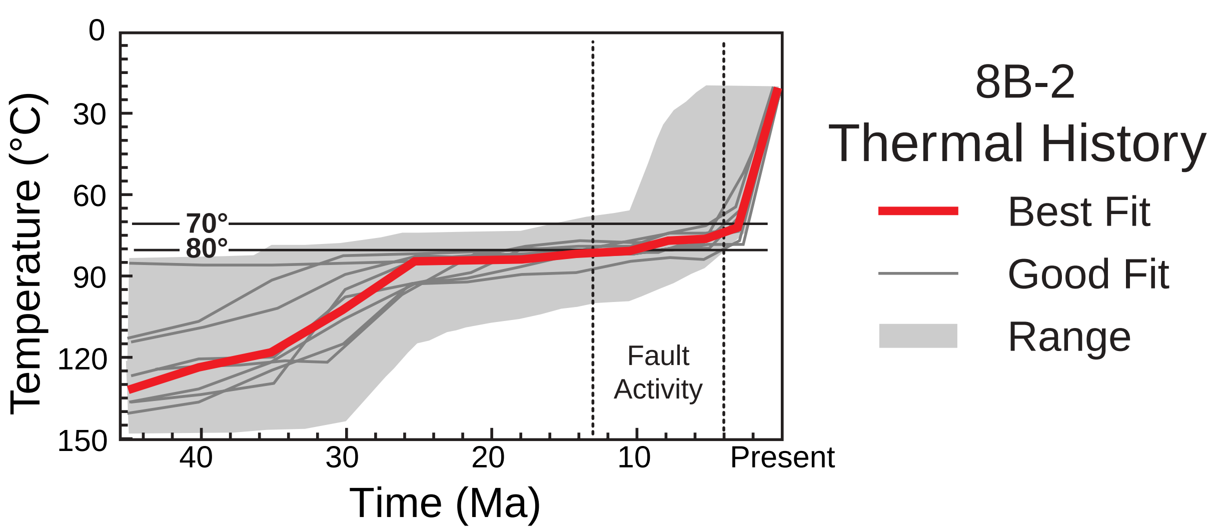

d'Alessio et al., 2003

Table DR1. Apatite Fission Track Analyses - San Gabriel Fault

Sample	Distance From Fault (m)	# Grains	Standard track density ($x10^6$ cm^{-2})	Fossil track density ($x10^4$ cm^{-2})	Induced track density ($x10^4$ cm^{-2})	Chi square prob. %	Central age (Ma)	Mean track length (μm)	Std. dev. (μm)
8b-1	-0.09	20	1.76	12.21	95.48	13	36.1 ± 4.8	12.5 ± 0.3	1.18
			(2866)	(82)	(641)			(14*)	
8b-2	-67	25	1.79	9.82	102.93	98	27.3 ± 3.4	11.3 ± 0.2	2.08
			(2911)	(77)	(807)			(118*)	
8b-4	0.50	33	2.24	26.1	152.2	95	61.3 ± 4.3	12.9 ± 0.3	1.04
			(3586)	(293)	(1705)			(15)	
8b-5	-9.0	20	1.85	12.2	117.1	92	30.8 ± 4.1	12.0 ± 0.9	2.44
			(2999)	(67)	(642)			(8)	
8b-6	-0.39	9	1.85	3.5	35.5	96	29.2 ± 10.2	11.1 ± 0.5	2.03
			(2999)	(9)	(91)			(20*)	
8b-7	0.02	40	2.28	34.5	304.7	99	41.2 ± 3.2	12.5 ± 0.2	0.67
			(3641)	(221)	(1950)			(20)	
8b-8	0.05	27	2.28	25.4	209.6	85	44.0 ± 3.5	12.6 ± 0.4	1.28
			(3641)	(215)	(1777)			(13)	
8b-9	0.10	29	2.31	29.5	222.4	92	48.8 ± 3.5		
			(3696)	(271)	(2044)				
8b-e	-0.06	20	2.08	12.6	107.4	77	38.9 ± 4.9	10.6 ± 0.4	0.96
			(3325)	(75)	(639)			(6*)	
8b-f	-0.03	20	2.06	21.3	166.2	38	41.2 ± 4.1		
			(3294)	(152)	(1188)				
8e-1	-0.04	20	1.91	11.4	109.5	94	31.6 ± 4.2	12.1 ± 0.2	1.48
			(3087)	(67)	(645)			(46*)	
8e-2	0.05	20	2.31	16.4	117.7	80	51.3 ± 5.6	12.5 ± 0.4	1.68
			(3696)	(105)	(753)			(22)	
8e-3	0.09	20	2.34	16.7	90.9	99	68.3 ± 7.7		
			(3752)	(102)	(556)				
8e-4	0.14	17	2.34	12.7	64.6	92	73.5 ± 8.7		
			(3752)	(93)	(471)				
8e-gouge	0	12	2.15	19.7	112.8	63	59.4 ± 7.0		
			(3441)	(97)	(556)				
8f-1	12.3	20	2.38	16.4	170.3	78	36.6 ± 3.9	12.7 ± 0.2	1.18
			(3807)	(105)	(1090)			(26)	
8f-2	70	20	2.38	10.2	76.3	98	50.5 ± 6.9	12.2 ± 0.2	1.60
			(3807)	(65)	(488)			(100)	

Distances shown are from the center of the ultracataclasite layer to the midpoint of the sample. Negative distances from the fault indicate samples on the granodiorite (south) side of the fault, while positive distances indicate samples from the gneiss (north) side. Samples were processed by d'Alessio and Donelick Analytical: standard magnetic and heavy liquid mineral separation processes were used. All samples were analyzed by Blythe. Apatites were mounted in epoxy. Sample surfaces were ground and polished. Apatite mounts were etched in 7% HNO_3 at 18°C for 22s. An "external detector" (e.g., Naeser, 1979), consisting of low-U (<5 ppb) Brazil Ruby muscovite, was used for each sample. Samples were irradiated in the Cornell University Triga nuclear reactor. Following irradiation, the muscovites were etched in 48% HF at 18°C for 30 min. Tracks were counted using a 100X dry lens and 1250X total magnification in crystals with well-etched, clearly visible tracks and sharp polishing scratches. A Kinitek stage and software written by Dumitru (1993) were used for analyses. Parentheses show number of tracks counted. Standard and induced track densities were determined on external detectors (geometry factor = 0.5), and fossil track densities were determined on internal mineral surfaces. Ages were calculated using zeta = 320 ± 9 for dosimeter glass SRM 962a (e.g., Hurford and Green, 1983). All ages are central ages, with the conventional method (Green, 1981) used to determine errors on sample ages. The chi-square test estimated the probability that individual grain ages for each sample belong to a single population with Poissonian distribution (Galbraith, 1981). * lengths were measured by Blythe on grains exposed to Cf –252 by Donelick Analytical.

Table DR2. Measured track lengths for all samples.

Sample #	bins (microns) 4-5	5-6	6-7	7-8	8-9	9-10	10-11	11-12	12-13	13-14	14-15	15-16	Mean length (#)	S.D.
8b-1							3	1	5	4			12.54 ± 0.32 (14)	1.18
8b-2		3	3	7	5	4	15	32	32	9	7	1	11.31 ± 0.19 (118)	2.08
8b-4							1	2	6	4	2		12.89 ± 0.27 (15)	1.04
8b-5					1	1	0	3	0	1	1	1	11.98 ± 0.86 (8)	2.44
8b-6				2	2	2	2	6	3	1	1	1	11.1 ± 0.45 (20)	2.03
8b-7								5	10	5			12.49 ± 0.15 (20)	0.67
8b-8							2	1	6	2	2		12.61 ± 0.36 (13)	1.28
8b-e						1	3	2					10.6 ± 0.39 (6)	0.96
8e-1						4	7	11	11	8	4	1	12.11 ± 0.22 (46)	1.48
8e-2					1	1	1	4	7	6	0	2	12.48 ± 0.36 (22)	1.68
8f-1							3	4	7	8	3	1	12.74 ± 0.23 (26)	1.18
8f-2	1	0	0	0	3	5	8	22	32	20	9		12.18 ± 0.16 (100)	1.60